Vesicle Size Distributions Measured by Flow Field-Flow Fractionation Coupled with Multiangle Light Scattering

Brian A. Korgel,* John H. van Zanten,# and Harold G. Monbouquette*

*Chemical Engineering Department, University of California Los Angeles, Los Angeles, California 90095-1592, and #Chemical Engineering Department, Johns Hopkins University, Baltimore, Maryland 21218 USA

ABSTRACT The separation method, flow field-flow fractionation (flow FFF), is coupled on-line with multiangle laser light scattering (MALLS) for simultaneous measurement of the size and concentration of vesicles eluting continuously from the fractionator. These size and concentration data, gathered as a function of elution time, may be used to construct both number- and mass-weighted vesicle size distributions. Unlike most competing, noninvasive methods, this flow FFF/MALLS technique enables measurement of vesicle size distributions without a separate refractive index detector, calibration using particle size standards, or prior assumptions about the shape of the size distribution. Experimentally measured size distributions of vesicles formed by extrusion and detergent removal are non-Gaussian and are fit well by the Weibull distribution. Flow FFF/MALLS reveals that both the extrusion and detergent dialysis vesicle formation methods can yield nearly size monodisperse populations with standard deviations of ~8% about the mean diameter. In contrast to the rather low resolution of dynamic light scattering in analyzing bimodal systems, flow FFF/MALLS is shown to resolve vesicle subpopulations that differ by much less than a factor of two in mean size.

INTRODUCTION

Unilamellar surfactant vesicles have long served as models for cell membranes (Johnson and Bangham, 1969) and more recently have been used as nanoscale vehicles for reagents in a wide variety of technologies, including drug delivery and targeting (Poste, 1980), medical imaging (Mauk and Gamble, 1979), nanocrystal formation (Korgel and Monbouquette, 1996; Fendler, 1987; Mann et al., 1986), separations (van Zanten and Monbouquette, 1992; van Zanten et al., 1995; Walsh and Monbouquette, 1993), and diagnostics (Jones et al., 1996). Vesicle size and size distribution are key parameters in most vesicle applications. For example, when used to deliver drugs, vesicle size and size distribution control, or have a strong impact on, dosage, targeting, and rate of clearance from the body (Litzinger et al., 1994). When used as reaction compartments for the synthesis of size-quantized nanocrystals whose optoelectronic properties are size-dependent, the vesicle size distribution must be as tight as possible, since it in turn governs the particle size distribution (Korgel and Monbouquette, 1996). Accurate estimation of ionophore- or ion channel-mediated ion permeability of vesicles also requires quantitative knowledge of the vesicle size and size distribution to calculate ion fluxes and permeabilities based on surface area (van Zanten and Monbouquette, 1992). Obviously, a strong need exists for rapid, dependable techniques to measure vesicle size and size distribution.

Although a variety of methods exist for measuring average vesicle size, few accurate, convenient, nondestructive methods for measuring the size distribution that do not require assumptions about the fundamental nature of the distribution are available (Moon and Giddings, 1993). Measurement methods include electron microscopy (e.g., cryo- and freeze-fracture TEM) (Hallett et al., 1991; Egelhaaf et al., 1996), sedimentation field-flow fractionation (Caldwell et al., 1981; Kirkland et al., 1982; Dreyer et al., 1988), nuclear magnetic resonance (NMR) spectroscopy (Hinton and Johnson, 1993), gel filtration chromatography (Lesieur et al., 1993), and static and dynamic light scattering (van Zanten, 1996). However, sample preparation for TEM can introduce artifacts and is destructive of the sample (Hallett et al., 1991; Egelhaaf et al., 1996). Sedimentation field-flow fractionation has proven to be a powerful technique for vesicle size distribution estimation, yet it requires a relatively complex centrifugation apparatus. Recent developments in HPLC-mode gel filtration chromatography for vesicle characterization may have overcome well-known shortcomings of this technique including limited fractionation range, long elution times, and lipid adsorption to the column (Lesieur et al., 1993). Nondestructive techniques based on dynamic light scattering (i.e., quasielastic light scattering, photon correlation spectroscopy) and NMR spectroscopy can yield accurate measures of the average vesicle size; however, in order to determine the size distribution, knowledge of its functionality unfortunately is required a priori. The determination of the size distribution using these latter methods is a mathematically ill-conditioned problem with no unique solution (Hinton and Johnson, 1993; McWhirter, 1980; Ostrowsky et al., 1981). The NMR technique

Received for publication 12 December 1997 and in final form 9 March 1998.

Address reprint requests to Dr. Harold G. Monbouquette, Chemical Engineering Department, UCLA, Los Angeles, CA 90095-1592. Tel.: 310-825-8946; Fax: 310-206-4107; E-mail: harold@seas.ucla.edu.

Brian A. Korgel's current address is Department of Chemistry, University College Dublin, Belfield, Dublin 4, Ireland.

0006-3495/98/06/3264/09 $2.00

and widely used dynamic light scattering methods rely on user input of the size distribution functional form and on the principle of parsimony, selection of the simplest solution that fits the data well. However, a complete understanding of the vesicle size distribution that results from various synthesis methods is not available; consequently, size distribution shape cannot be measured unambiguously using these techniques. A convenient nondestructive method for measuring absolute vesicle size distributions without any prior assumptions on their functionality therefore remains an unfilled need.

In this report we demonstrate that by coupling the separation method, flow field-flow fractionation (flow FFF), with continuous-flow multiangle laser light scattering (MALLS), the absolute size distribution of phosphatidylcholine (PC) vesicles can be measured conveniently without any prior assumptions about the nature of the distribution. Flow FFF is one of a family of FFF techniques where particles or macromolecules are separated in a thin rectangular channel by applying an appropriate field (e.g., flow, electrical, thermal) orthogonal to the channel flow, which under normal operating conditions results in longer retention times for larger macromolecules or colloids (Giddings, 1995). Fractions eluting from the FFF chamber may be fed continuously to a detector for analysis. Moon and Giddings (1993) demonstrated the efficacy of flow FFF for measuring surfactant vesicle size distributions. However, they used a UV detector to monitor the eluent and correlated time of elution to size based on the measured elution time of latex bead size standards. The UV detector simply measured turbidity that was not corrected for the dependence of light scattering on vesicle size, thus smaller particles were underrepresented in their mass-weighted size distributions. Others have coupled flow FFF, a MALLS instrument and a refractive index (RI) detector to determine macromolecule and polymer particle size distributions (Thielking and Kulicke, 1996; Thielking et al., 1995; Roessner and Kulicke, 1994; Wittgren and Wahland, 1997). In these studies, macromolecule or colloid size and concentration were determined separately by the MALLS instrument and RI detector, respectively. Wyatt and Villalpando (1997) recently gave a brief description, without theoretical arguments, of the use of flow FFF followed by MALLS to determine the number-weighted size distribution of polymeric particle size standards. We describe below the theoretical basis for use of MALLS to measure *simultaneously* the size and concentration of eluting vesicles such that *both* absolute number- and mass-weighted vesicle size distributions can be determined without an RI detector, prior calibration using particle size standards, or assumptions about the nature of the size distribution. We examine vesicles made using extrusion and detergent depletion methods and demonstrate that this technique holds promise for the determination of both unimodal and bimodal size distributions at higher resolution than that attained using dynamic light scattering.

THEORETICAL CONSIDERATIONS

Flow field-flow fractionation

Flow FFF separates particles based on size. The sample is injected into a narrow rectangular chamber where the two larger opposite walls consist of solvent permeable membranes that completely reject the particles of interest. A set channel volumetric flow, v_c, tangential to the membrane walls, carries the sample through the chamber while a transmembrane cross-flow, v_x, imposes a Stokes drag force that impinges the particles against the channel wall. The effect of the cross-flow on the vesicle elution time is dependent on the diameter of the particles. The drag on the smaller vesicles is less and their Brownian motion is greater, thus they tend to elute first from the fractionator. The vesicle elution time, t_r, depends on v_c, v_x, the channel width, w, and the vesicle diffusion coefficient, D_v (Liu et al., 1991; Moon and Giddings, 1993)

$$t_r \approx \frac{w^2 v_x}{6 D_v v_c} = \frac{\pi \eta w^2 v_x}{2kT v_c} d, \tag{1}$$

where η is the solvent viscosity, k is Boltzmann's constant, T is the temperature, and d is the vesicle diameter. Since the vesicle diffusion coefficient is inversely proportional to the vesicle diameter, retention time is directly proportional to vesicle diameter.

Light scattering theory

An expression for the vesicle number concentration may be derived from the expression of Zimm (1948) based on the fluctuation theory of light scattering,

$$R_\theta \approx K c_v M_v P(\theta)[1 - 2A_2 c_v M_v P(\theta)], \tag{2}$$

where c_v is the vesicle concentration; M_v is the vesicle molecular weight; $P(\theta)$ is the shape factor, which relates vesicle size and shape to the angular dependence of scattered light intensity; R_θ is the Rayleigh ratio; A_2 is the second virial coefficient; and K is the scattering coefficient,

$$K = \frac{2\pi^2 n_s^2}{\lambda^4 N_A}\left(\frac{\partial n}{\partial c_v}\right)^2. \tag{3}$$

For a vertically polarized laser such as that used in this study, $R_\theta = I(\theta) r^2 / I_o V$, where r is the distance from the scatterer, I_o is the incident intensity, and V is the scattering volume. In Eq. 3, $\partial n/\partial c_v$ is the change in dispersion refractive index with vesicle concentration, λ is the wavelength of light, n_s is the solvent refractive index, and N_A is Avogadro's number. Since $c_v = n_v M_v / N_A$, where n_v is the vesicle number concentration, Eq. 2 can be rearranged to give an expression for n_v,

$$n_v = \frac{R_\theta N_A}{K M_v^2 P(\theta)}\left[\frac{1}{1 - 2A_2 c_v M_v P(\theta)}\right]. \tag{4}$$

If it is assumed that size monodisperse fractions elute from the flow field-flow fractionator, it is a simple matter to reconstruct the vesicle number distribution. The number fraction of vesicles in fraction i can be calculated from

$$\frac{N_{v,i}}{N_{v,total}} = \frac{\dfrac{R_{\theta,i}}{M_{v,i}^2 P_i(\theta)}\left[\dfrac{1}{1 - 2A_{2,i}c_{v,i}M_{v,i}P_i(\theta)}\right]}{\displaystyle\sum_i \frac{R_{\theta,i}}{M_{v,i}^2 P_i(\theta)}\left[\frac{1}{1 - 2A_{2,i}c_{v,i}M_{v,i}P_i(\theta)}\right]}. \quad (5)$$

where $N_{v,i}$ is the number of vesicles in fraction i.

Up to this point, the derivation actually is general for colloidal and macromolecular systems in the single contact approximation (Zimm, 1948). The following simplification and the choice of shape factor are what limit this analysis to unilamellar spherical vesicles that are no more than ~200 nm in diameter. However, a number of shape factors have been derived for other systems (van Zanten, 1996). Given that a Zimm plot analysis yields $A_2 = -1.0 \pm 0.5 \times 10^{-4}$ mol ml/g^2 for the liposome dispersions under consideration in this report, and that the typical vesicle concentration in a given eluted fraction is at most of order 10^{-6} g/ml, Eq. 5 can be simplified to give

$$\frac{N_{v,i}}{N_{v,total}} \approx \frac{I_i(\theta)/M_{v,i}^2 P_i(\theta)}{\displaystyle\sum_i I_i(\theta)/M_{v,i}^2 P_i(\theta)}. \quad (6)$$

To calculate $N_{v,i}/N_{v,total}$, the shape factor and the molecular weight must be determined for each fraction. Values for the shape factor are calculated from scattered light intensity measurements given an appropriate model for light scattering by PC vesicles and that $I(\theta) \propto P(\theta)$ for the very dilute solutions assumed here. We previously have shown that PC vesicles <~120 nm in diameter scatter within the Rayleigh-Gans-Debye (RGD) approximation (van Zanten and Monbouquette, 1991, 1994; van Zanten, 1996) according to the shape factor for a hollow sphere (Kerker, 1969)

$$P(\theta) = \left[\frac{3}{q^3(R_o^3 - R_i^3)}(\sin qR_o - qR_o \cos qR_o - \sin qR_i + qR_i \cos qR_i)\right]^2, \quad (7)$$

where q is the scattering vector,

$$q = \frac{4\pi n_s}{\lambda_o}\sin\left(\frac{\theta}{2}\right),$$

and R_i and R_o are the inner and outer vesicle radii. Assuming a vesicle bilayer thickness, Eq. 7 can be fit to light scattering data and R_o can be estimated. However, for this work it was found to be unnecessary to fit the shape factor to the light scattering data for each fraction; rather, the dissymmetry between the intensities at 135° and 69°, $I(135°)/I(69°)$, is set equal to $P(135°)/P(69°)$ and solved for R_o using an estimated wall thickness of 3.4 nm for PC vesicles (van Zanten, 1994).

Given the vesicle size for each fraction, the apparent vesicle molecular weight is calculated using the volume per lipid molecule, $\tilde{v}$, and the molecular weight of the lipid, M_l, or the lipid bilayer mass density, ρ_b,

$$M_v = \frac{4\pi}{3\tilde{v}}(R_o^3 - R_i^3)M_l = \frac{4\pi}{3}(R_o^3 - R_i^3)N_A\rho_b. \quad (8)$$

Although ρ_b may be determined by using hydrodynamic methods (Huang and Mason, 1978), an estimate of 1 g/cm^3 likely is very good for most surfactant vesicles and is within 2% of the experimentally determined value for egg PC vesicles of 1.015 g/ml (Huang and Mason, 1978). Once the relative number of vesicles in each eluted fraction and the size of these vesicles are calculated from the light scattering data, a number-weighted vesicle size histogram may be constructed.

From such a histogram, the light scattering behavior of the original unfractionated sample can be reconstructed using the following equation:

$$\frac{I(\theta)}{I(\theta_r)} = \frac{\displaystyle\sum_i P_i(\theta)(N_{v,i}/N_{v,total})M_{v,i}^2}{\displaystyle\sum_i P_i(\theta_r)(N_{v,i}/N_{v,total})M_{v,i}^2}, \quad (9)$$

which follows from the direct relationship between $I(\theta)$ and $P(\theta)$. Here, θ_r is the reference angle corresponding to which the scattered light intensity is normalized. This expression provides a convenient means to check the accuracy of the histograms generated by using flow FFF/MALLS and the data analysis described above.

Mass-weighted size distributions were not calculated for the vesicle populations studied in this work, yet a similar derivation to that given above can be used to arrive at an expression for the mass fraction of vesicles that elute with each volume fraction from the flow FFF unit,

$$\frac{m_{v,i}}{m_{v,total}} = \frac{I_i(\theta)/P_i(\theta)M_{v,i}}{\displaystyle\sum_i I_i(\theta)/P_i(\theta)M_{v,i}}. \quad (10)$$

Here, $m_{v,i}$ is the mass of vesicles in fraction i. Alternatively, the mass-weighted size distribution could be generated indirectly from the information in the number-weighted size distribution.

EXPERIMENTAL PROCEDURES

Vesicle preparation

Small unilamellar L-α-phosphatidylcholine (egg lecithin, Avanti Polar Lipids, Alabaster, AL) vesicles are prepared by extrusion (Hope et al., 1985; Olson et al., 1979) or detergent dialysis (Kagawa and Racker, 1971; Brunner et al., 1976; Milsmann et al., 1978). In preparation for extrusion, an ethanolic lipid solution is dried for at least 4 h at reduced pressure using a rotary evaporator at 40°C. The dried lipid film is rehydrated with 200 mM NaCl to give a 20 mg/ml dispersion. Subsequently, this dispersion is

extruded (12 passes) using a 10-ml thermobarrel extruder (Lipex Biomembranes, Vancouver) at 600 psi and room temperature through 30-, 50-, or 100-nm pore diameter Nucleopore polycarbonate membranes (Corning Costar Corp., Cambridge, MA) to form vesicles.

Vesicles are formed by detergent removal using either the non-ionic detergent, *n*-hexyl-β-D-glucopyranoside (HXG) (0.05 lipid/detergent mole ratio), or sodium cholate (0.65 lipid/detergent mole ratio), both from Sigma (St. Louis, MO). Before detergent dialysis, ethanolic solutions of PC and detergent are dried as above. The dried films are rehydrated with 200 mM NaCl (HXG/PC) or 50 mM NaCl (sodium cholate/PC) solution to give a final lipid concentration of 20 mg/ml. Vesicles are formed by dialyzing the lipid/detergent mixture against 200 mM NaCl or 50 mM NaCl for 24 h using dialysis tubing with a molecular weight cutoff of 6–8,000 (Spectrum Medical Industries, Los Angeles, CA).

Flow field-flow fractionation and light scattering

Before separation in the flow field-flow fractionator (FFFractionation, Salt Lake City, UT), vesicle dispersions are diluted with 200 mM NaCl to 10 mg/ml lipid concentrations to avoid detector saturation and are filtered using a 0.45-μm pore filter. Samples (20 μl) are injected in stopped flow mode and subsequently are carried by saline mobile phase (200 mM NaCl) through the FFF chamber (28.5 cm long, 2.0 cm wide, and 0.25 mm thick) at a flow rate of 1.75 ml/min. The cross-flow flow rate is set at 0.6–0.67 ml/min. At our injected concentrations, band broadening effects are negligible based on measurements of monodisperse latex particles (data not shown). A typical separation is completed in 15–20 min.

The fractionator is coupled to the Dawn B/F Laser Photometer (Wyatt Technology, Inc., Santa Barbara, CA) using the flow-through light scattering cell. The laser is a vertically polarized 5 mW He-Ne laser with a wavelength in vacuo of 632.8 nm. Scattered light intensities can be measured by fixed detectors at up to 18 scattering angles ranging from 3° to 158°; however, in the flow-cell configuration, the first four detectors at the smallest scattering angles, and the 18th detector at the largest scattering angle, cannot be used due to Snell's law limitations and reflection effects. Light scattering data are collected every second of run time at a gain of 100.

Batch static light scattering measurements on unseparated samples are conducted using a scintillation vial in the Dawn instrument (van Zanten and Monbouquette, 1991, 1994; van Zanten, 1994). Approximately 10 μl of the 20 mg PC/ml vesicle dispersion is added to 10 ml of 200 mM NaCl solution for these measurements.

RESULTS AND DISCUSSION

Size distribution determination

The data presented in Fig. 1 for vesicles formed by extrusion through 100 nm pore membranes illustrate the dual use of the continuous flow static light scattering instrument to determine both the relative number and absolute size of vesicles eluting from the FFF chamber. The scattered light intensity at 69° for each eluted volume fraction relative to the sum of the scattered light intensities for all fractions is compared to $N_{v,i}/N_{v,total}$, which is calculated using the vesicle radii determined for each fraction and Eq. 5. This comparison illustrates the functional dependence of scattered light intensity on both vesicle size and concentration. Larger vesicles scatter more light, thus the peak in the intensity data is shifted to longer retention time relative to the number density data.

Subsequent to the early burst of apparently larger vesicles, the vesicle size increases steadily with elution time, as

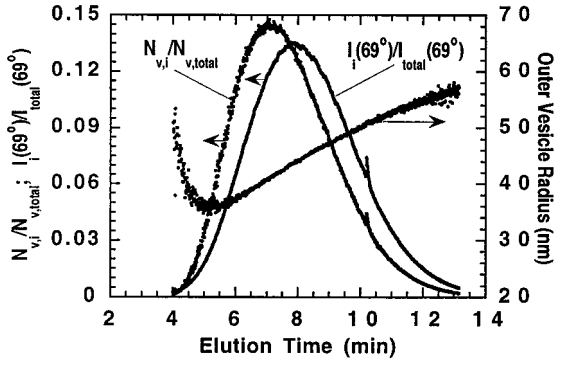

FIGURE 1 The relative scattered light intensity, vesicle number fraction, and radius versus elution time.

expected (Fig. 1). The slope of vesicle radius versus t_r from this nearly linear region in Fig. 1 is estimated at 2.8 nm/min and is close to that expected based on Eq. 1 (3.2 nm/min), which confirms that the vesicles are separated based on the published theory. A likely explanation for the apparent burst of larger vesicles at short elution time may be inaccurate light scattering data at the very low vesicle concentrations of the early fractions. The vesicles in these samples are too small to exhibit the "steric-hyperlayer mode" of flow FFF, where large particles get swept into the parabolic channel flow field and elute early (Jensen et al., 1996). Also, the system automatically stops channel flow briefly after injection to allow time for the sample to come to equilibrium against the channel wall before elution. More detailed research is underway to determine the exact nature of this artifact. In any case, the number fraction is so low at early elution times that these data have a very small impact on the measured size distribution.

In Fig. 2, the measured scattered light intensities are normalized to the intensity at the 35° detector for five

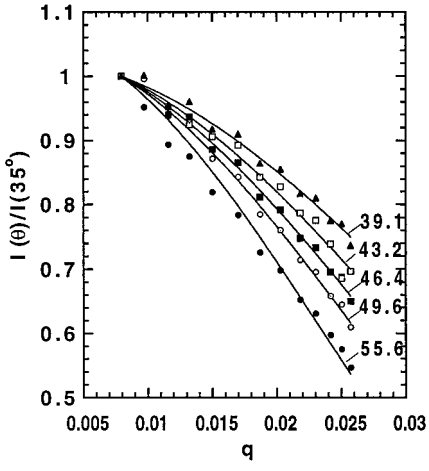

FIGURE 2 The scattered light intensity normalized to the 35° detector versus q for five fractions analyzed at the following elution times (min): (▲), 6.3; (□), 7.4; (■), 8.6; (○), 9.7; (●), 10.9. The curves represent the RGD approximation for hollow spheres fit to the scattering data. Also shown is the corresponding outer vesicle radius (nm).

different elution volumes and are plotted versus the scattering vector, q. In this work, 13 scattering angles from 35° to 132° are used and show good precision. For most fractions, solid curves representing the best fit of the shape factor overlay the scattering data well, which indicates that these vesicles scatter light within the RGD approximation, that they remain approximately spherical in the flow field, and that significant flow-induced aggregation does not occur.

Fig. 3 shows the number-weighted size distribution constructed from the static light scattering measurements presented in Figs. 1 and 2. As a test of the accuracy of the size distribution shown in Fig. 3, the total static light scattering behavior of the vesicle population represented by the flow FFF/MALLS histogram can be reconstituted using Eq. 9 and compared to the actual batch static light scattering measured for the unseparated vesicle dispersion. A fit of the shape factor from RGD theory for hollow spheres, assuming a monodisperse sample, to the unseparated dispersion gives an average vesicle radius of 42.5 nm (see Fig. 4), in close agreement with the peak radius of the histogram (Fig. 3) obtained using flow FFF/MALLS. The angular dependence of scattered light intensity for the unfractionated vesicle population reconstructed from the FFF histogram in Fig. 3 nearly superimposes the actual batch data, strongly suggesting that this flow FFF/MALLS technique provides an accurate measure of the vesicle size distribution.

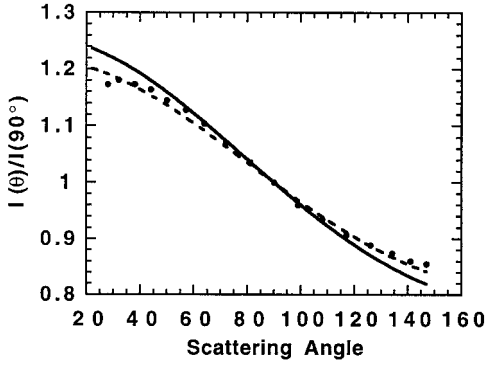

FIGURE 4 Batch static light scattering measurements for a vesicle population formed by extrusion through a 100-nm pore membrane before separation by flow FFF (●). The curves correspond to the RGD approximation for hollow spheres fit to the batch scattering data (- - -) and to the expected scattering from the unfractionated sample calculated using the size distribution measured by flow FFF/MALLS (—).

Comparison of detergent depletion and extrusion vesicles

Significant controversy persists regarding the expected shape of vesicle size distributions and their dependence, if any, on vesicle formation method and conditions. The major obstacle encountered when addressing this issue has been a lack of an accurate and convenient means to measure absolute vesicle size distributions. Figs. 5-8 show additional measured size distributions obtained using flow FFF/MALLS for vesicles synthesized by extrusion or detergent depletion. The vesicles in Figs. 5 and 6 were formed by extrusion through 50- and 30-nm pores, respectively, whereas the vesicles in Figs. 7 and 8 were formed by dialysis of HXG and cholate mixed detergent/lipid micelles, respectively. It is apparent immediately that these asymmetric size distributions are non-Gaussian. Similar asymmetric size distributions have been observed previously for vesicles made by sonication (Tenchov et al., 1985; Tenchov and Yanev, 1986), solvent evaporation (Moon and Giddings, 1993), extrusion (White et al., 1996), and detergent depletion (Rotenberg and Lichtenberg, 1990; Egelhaaf et al., 1996) using a variety of techniques, including dynamic light scattering (Rotenberg and Lichtenberg, 1990; Egelhaaf et al., 1996). These similarities in the shape of vesicle size distributions may lend support to hypotheses that these vesicle preparation methods share a common mechanism for vesicle formation based on, for example, the aggregation of small, discoid lipid micelles (Pansu, 1990; Tenchov et al., 1985; Lasic, 1987, 1988; Fromherz, 1983; Fromherz and Rüppel, 1985; Fromherz et al., 1986). The sharpness and skewed nature of the vesicle populations formed by deter-

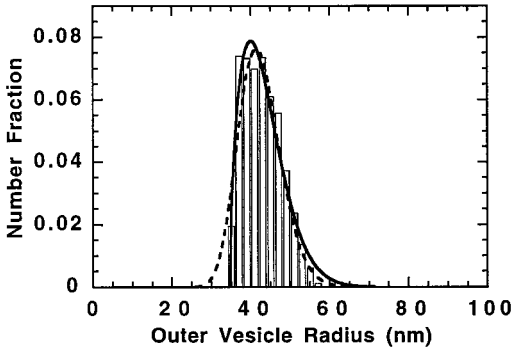

FIGURE 3 Number-weighted size distribution of vesicles formed by extrusion through a 100-nm pore membrane. The solid curve corresponds to the Weibull distribution fit, whereas the dashed curve represents the best log-normal distribution fit.

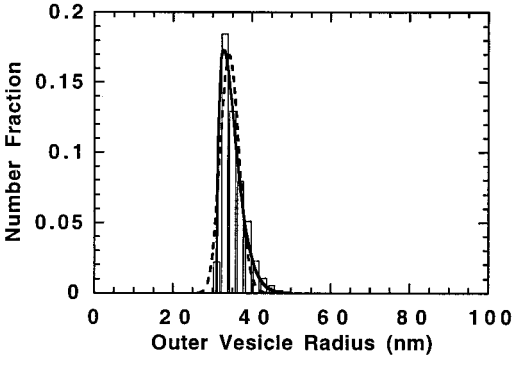

FIGURE 5 Number-weighted size distribution of vesicles formed by extrusion through a 50-nm pore membrane. The solid curve corresponds to the Weibull distribution fit, whereas the dashed curve represents the best log-normal distribution fit.

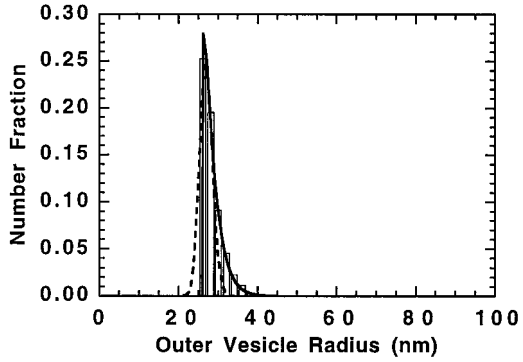

FIGURE 6 Number-weighted size distribution of vesicles formed by extrusion through a 30-nm pore membrane. The solid curve corresponds to the Weibull distribution fit, whereas the dashed curve represents the best log-normal distribution fit.

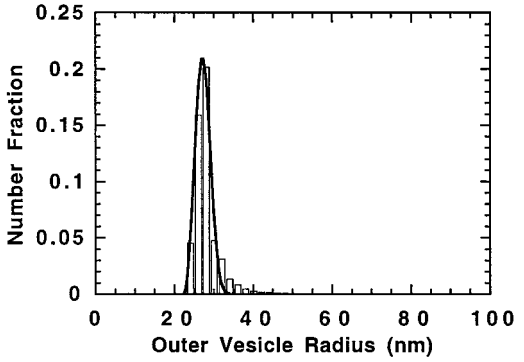

FIGURE 8 Number-weighted size distribution of the vesicles formed by detergent depletion using cholate. The solid curve corresponds to the Weibull distribution fit.

gent dialysis and by extrusion through 30- and 50-nm pore membranes (Figs. 5–8) limits the nature of size distribution functions that can fit the data well. As shown in Fig. 3 and in Figs. 5–8, a simple log-normal function cannot capture the sharp features of the measured distribution, particularly the steepness of the data at smaller diameters. However, the lower-end truncation of the size distribution may be exaggerated by incomplete fractionation and inaccurate sizing of the smaller vesicles in the distribution (see the earlier discussion and Fig. 1).

Tenchov et al. (1985; Tenchov and Yanev, 1986) have shown that a uniform random fragmentation model leads to a predicted size distribution for vesicles formed by sonication, for example, which is identical to the Weibull extremal probability distribution,

$$f(d) = \frac{\delta}{\eta}\left(\frac{d - d_o}{\eta}\right)^{\delta-1} \exp\left[-\left(\frac{d - d_o}{\eta}\right)^{\delta}\right], \qquad (11)$$

where d is the vesicle diameter. The distributions of Fig. 3 and Figs. 5–8 are fit well by this three-parameter (d_o, δ, η) function (see Table 1), whereas the log-normal distribution, which arises from a closely related model of random fragmentation (Tenchov and Yanev, 1986), cannot describe the data well. In fact, the sum of the squares of the residuals (χ^2) is about an order of magnitude or more greater for the best log-normal fits obtained in all cases. However, given the simplicity of the uniform random fragmentation model, only tenuous physical meaning can be assigned to the Weibull distribution parameters. Tenchov et al. (1985; Tenchov and Yanev, 1986) define d_o as the minimum vesicle diameter, relate η to the efficiency of the lipid membrane fragmentation process (η decreases with increasing shearing efficiency), and represent δ as the dimensionality of the reclosing process or the vesicle formation process with 1 being linear, 2 being planar, and 3 being spherical. As the dimensionality increases, the distribution becomes increasingly Gaussian in shape; when δ equals one, the distribution becomes a simple exponential.

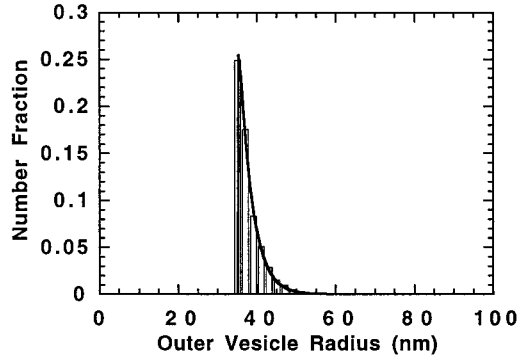

FIGURE 7 Number-weighted size distribution of the vesicles formed by detergent depletion using HXG. The solid curve corresponds to the Weibull distribution fit.

In Table 1 the Weibull distribution parameters are given for each of the vesicle populations measured. The physical meaning assigned to d_o is brought into doubt by the wide range of values obtained with the same phospholipid under the different vesicle formation conditions used, and the fact that egg lecithin vesicles with much smaller diameter than the d_o values listed here have been achieved by others (Rotenberg and Lichtenberg, 1990). However, the observation that vesicles made by extrusion through the 30- and 50-nm pores have significantly larger mean diameters than the membrane pores suggests that the vesicles are formed by extrusion-induced lipid aggregate fragmentation followed by reassembly into vesicles. The parameter, η, decreases significantly with decreasing pore size, as expected given its definition above as a measure of lipid membrane fragmentation. Increased shearing efficiency (smaller η) results in the observed tightening of the size distribution with the smaller pore sizes. The initial slope of the size distribution also increases with decreased pore size, as reflected by decreased δ, which approaches the limiting value of one for the smaller pore size extrusion membranes.

Although the Weibull function fits the size distribution data for detergent dialysis vesicles well, assignment of meaning to the distribution parameters in the spirit of the analysis of Tenchov et al. (1985; Tenchov and Yanev, 1986)

TABLE 1 Parameters for Weibull distribution fits to number fraction histograms of vesicle diameter

Vesicle Sample	δ*	η	d_o	d_{max}[#]	d_{mean}	σ[§]	χ^2[¶]
100-nm extrusion	1.62	19.4	69.3	80.1	86.7	11.0	11
50-nm extrusion	1.43	8.5	62.0	65.7	69.7	5.5	11
30-nm extrusion	1.10	5.6	51.9	52.6	57.3	4.9	3
Cholate dialysis	2.94	11.0	44.8	54.3	54.6	3.6	48
HXG dialysis	1.03	6.5	70.0	70.2	76.4	6.3	3

Fits were conducted with the NonlinearFit package of Mathematica v2.2 (Wolfram Research, Champaign, IL).
* Fit was limited to $1 < \delta < 3$.
[#] Maximum value of d of the Weibull fit.
[§] Standard deviation.
[¶] Sum of the squares of the residuals ($\times 10^5$).

is less straightforward. The vesicles formed using cholate shown in Fig. 8 are smaller than those formed using HXG (Fig. 7) in agreement with an earlier comparison of vesicles formed using cholate and another glucoside detergent, octyl glucoside (Rotenberg and Lichtenberg, 1990). The differences in vesicle size obtained using these two detergents has been ascribed to differences both in rates of detergent removal and in rates of detergent-enhanced vesicle fusion just subsequent to vesiculation when substantial detergent still remains (Rotenberg and Lichtenberg, 1990). A number of groups (Rotenberg and Lichtenberg, 1990; Fromherz, 1983; Pansu, 1990; Lasic, 1987) have accepted a common view that vesicle formation by detergent depletion begins as the removal of detergent results in exposure of hydrophobic phospholipid tails at the edges of small, discoid micelles. These micelles aggregate to reduce edge energy until a critical micelle size or detergent-to-lipid ratio is reached where, upon further detergent removal, it becomes energetically more favorable to curl into a closed vesicle and eliminate edges at the expense of increased curvature elastic energy. The initial cholate/PC micelles are known to be smaller than those of HXG/PC, which superficially might suggest a lower η for the cholate/PC system, yet the reverse is true (Table 1). The random uniform fragmentation model of Tenchov et al. (1985; Tenchov and Yanev, 1986) incorporates very little of the relevant physics and thermodynamics governing the process of vesicle formation, particularly by detergent depletion. Although the Weibull distribution function describes vesicle size distributions well, this observation cannot be taken in and of itself as confirmation of the model of Tenchov et al. (1985; Tenchov and Yanev, 1986) since concrete physical meaning of all the distribution function parameters is not available.

Bimodal distribution

To further illustrate the power of this technique for determining vesicle size distributions, a mixture of vesicles of different average size are analyzed by flow FFF/MALLS. The size distribution corresponding to a 4:1 by volume mixture of the vesicle samples produced by sodium cholate and HXG removal, respectively, is shown in Fig. 9. Two peaks in vesicle radius are resolved with only an 8-nm separation. The peaks of the two modes of the distribution occur at 27 nm and 36 nm, very close to the peaks in the histograms of the two original vesicle samples (see Figs. 7 and 8). The resolution of this bimodal size distribution illustrates the possible superiority of flow FFF/MALLS for resolving heterogeneous populations. In comparison, dynamic light scattering (DLS) alone cannot resolve peaks in a bimodal distribution corresponding to less than a factor of two in size (Kölchens et al., 1993). If DLS could be coupled effectively to a flow FFF device, improved resolution might be achievable. However, the explicit time dependence of DLS makes it more amenable to batch as opposed to flow measurements, and a fast cumulants method might require higher particle concentrations than can be separated well by flow FFF.

CONCLUSIONS

Flow FFF/MALLS enables the rapid, convenient, and noninvasive measurement of vesicle size distributions without prior calibration using size standards or assumptions about the shapes of the distributions. The high resolution of the technique will make it particularly useful for the measurement of multimodal distributions. With further refinement and its use in well controlled experiments, flow FFF/MALLS may provide the tool necessary to connect theoret-

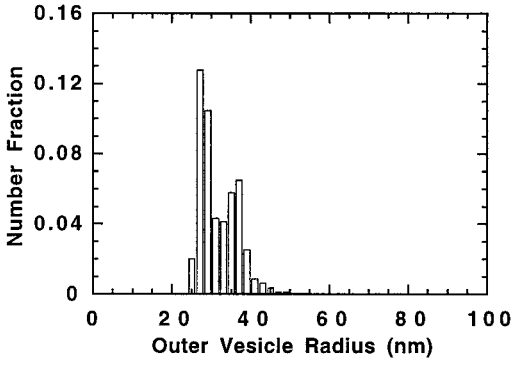

FIGURE 9 Number-weighted size distribution of the mixture of vesicles formed by dialysis with cholate and HXG (4:1 volume ratio cholate/HXG vesicles).

ical prediction of vesicle size distributions (Tenchov and Yanev, 1986; Tenchov et al., 1985; Kegel and Reiss, 1996) with experimental measurements.

The authors thank Shashi K. Murthy and Damien C. Nevoret for their assistance with the flow FFF measurements at Johns Hopkins. The authors benefited from illuminating scientific discussions with Philip J. Wyatt (Wyatt Technology, Inc., Santa Barbara, CA).

This project was supported by the National Science Foundation and the US Environmental Protection Agency (Award CTS-9525019). B.A.K. is grateful for a US Department of Education Pollution Prevention Fellowship (Award P200A40732).

REFERENCES

Brunner, J., P. Skrabal, and H. Hauser. 1976. Single bilayer vesicles prepared without sonication physico-chemical properties. *Biochim. Biophys. Acta.* 455:322–331.

Caldwell, K. D., G. Karaiskakis, and J. C. Giddings. 1981. Characterization of liposomes by sedimentation field-flow fractionation. *Colloids Surf.* 3:233–238.

Dreyer, R., E. Hawrot, A. C. Sartorelli, and P. P. Constantinides. 1988. Sedimentation field flow fractionation of fused unilamellar vesicles: comparison with electron microscopy and gel filtration. *Anal. Biochem*. 175:433–441.

Egelhaaf, S. U., E. Wehrli, M. Müller, M. Adrian, and P. Schurtenberger. 1996. Determination of the size distribution of lecithin liposomes: a comparative study using freeze fracture, cryoelectron microscopy and dynamic light scattering. *J. Microscopy*. 184:214–228.

Fendler, J. H. 1987. Atomic and molecular clusters in membrane mimetic chemistry. *Chem. Rev.* 87:877–899.

Fromherz, P. 1983. Lipid-vesicle structure: size control by edge-active agents. *Chem. Phys. Lett.* 94:259–266.

Fromherz, P., C. Röcker, and D. Rüppel. 1986. From discoid micelles to spherical vesicles: the concept of edge energy. *Faraday Discuss. Chem. Soc.* 81:39–48.

Fromherz, P., and D. Rüppel. 1985. Lipid vesicle formation: the transition from open disks to closed shells. *FEBS Lett.* 179:155–159.

Giddings, J. C. 1995. Measuring colloidal and macromolecular properties by FFF. *Anal. Chem.* 67:592A–598A.

Hallett, F. R., B. Nickel, C. Samuels, and P. H. Krygsman. 1991. Determination of vesicle size distributions by freeze-fracture electron microscopy. *J. Elec. Micros. Technique.* 17:459–466.

Hinton, D. P., and C. S. Johnson, Jr. 1993. Diffusion ordered 2D NMR spectroscopy of phospholipid vesicles: determination of vesicle size distributions. *J. Phys. Chem.* 97:9064–9072.

Hope, M. J., M. B. Bally, G. Webb, and P. R. Cullis. 1985. Production of large unilamellar vesicles by a rapid extrusion procedure. Characterization of size distribution, trapped volume and ability to maintain a membrane potential. *Biochim. Biophys. Acta.* 812:55–65.

Huang, C., and J. T. Mason. 1978. Geometric packing constraints in egg phosphatidylcholine vesicles. *Proc. Natl. Acad. Sci. USA.* 75:308–310.

Jensen, K. D., S. K. R. Williams, and J. C. Giddings. 1996. High-speed particle separation and steric inversion in thin flow field-flow fractionation channels. *J. Chromatogr. A.* 746:137–145.

Johnson, S. M., and A. D. Bangham. 1969. Potassium permeability of single compartment liposomes with and without valinomycin. *Biochim. Biophys. Acta.* 193:82–91.

Jones, M. A., P. K. Kilpatrick, and R. G. Carbonell. 1996. Competitive immunosorbent assays using ligand-enzyme conjugates and bifunctional liposomes—theory and experiment. *Biotechnol. Prog*. 12:519–526.

Kagawa, Y., and E. Racker. 1971. Partial resolution of the enzymes catalyzing oxidative phosphorylation. XXV. Reconstitution of vesicles catalyzing $^{32}P_i$-adenosine triphosphate exchange. *J. Biol. Chem*. 246: 5477–5487.

Kegel, W. K., and H. Reiss. 1996. Theory of vesicles and droplet type microemulsions: configurational entropy, size distribution, and measurable properties. *Ber. Bunsenges. Phys. Chem.* 100:300–312.

Kerker, M. 1969. The Scattering of Light and Other Electromagnetic Radiation. Academic Press, New York.

Kirkland, J. J., W. W. Yau, and F. C. Szoka. 1982. Sedimentation field flow fractionation of liposomes. *Science*. 215:296–298.

Kölchens, S. V., V. Ramaswami, J. Birgenheier, L. Nett, and D. F. O'Brien. 1993. Quasi-elastic light scattering determination of the size distribution of extruded vesicles. *Chem. Phys. Lipids*. 65:1–10.

Korgel, B. A., and H. G. Monbouquette. 1996. Synthesis of size-monodisperse CdS nanocrystals using phosphatidylcholine vesicles as true reaction compartments. *J. Phys. Chem.* 100:346–351.

Lasic, D. D. 1987. A general model of vesicle formation. *J. Theor. Biol.* 124:35–41.

Lasic, D. D. 1988. The mechanism of vesicle formation. *Biochem. J.* 256:1–11.

Lesieur, S., C. Grabielle-Madelmont, M. Paternostre, and M. Ollivon. 1993. Study of size distribution and stability of liposomes by high performance gel exclusion chromatography. *Chem. Phys. Lipids*. 64: 57–82.

Litzinger, D. C., A. M. J. Buiting, N. van Rooijen, and L. Huang. 1994. Effect of liposome size on the circulation time and intraorgan distribution of amphipathic poly(ethylene glycol)-containing liposomes. *Biochim. Biophys. Acta*. 1190:99–107.

Liu, M.-K., P. S. Williams, M. N. Myers, and J. C. Giddings. 1991. Hydrodynamic relaxation in flow field-flow fractionation using both split and frit inlets. *Anal. Chem.* 63:2115–2122.

Mann, S., J. P. Hannington, and R. J. P. Williams. 1986. Phospholipid vesicles as a model system for biomineralization. *Nature*. 324:565–567.

Mauk, M. R., and R. C. Gamble. 1979. Preparation of lipid vesicles containing high levels of entrapped radioactive cations. *Anal. Biochem.* 94:302–307.

McWhirter, J. G. 1980. A stabilized model-fitting approach to the processing of laser anemometry and other photon correlation data. *Opt. Acta*. 27:83–105.

Milsmann, M. H. W., R. A. Schwendener, and H.-G. Weder. 1978. The preparation of large single bilayer liposomes by a fast and controlled dialysis. *Biochim. Biophys. Acta.* 512:147–155.

Moon, M. H., and J. C. Giddings. 1993. Size distribution of liposomes by flow field-flow fractionation. *J. Pharm. Biomed. Anal.* 11:911–920.

Olson, F., C. A. Hunt, F. C. Szoka, W. J. Vail, and D. Papahadjopoulos. 1979. Preparation of liposomes of defined size distribution by extrusion through polycarbonate membranes. *Biochim. Biophys. Acta*. 557:9–23.

Ostrowsky, N., D. Sornette, P. Parker, and E. R. Pike. 1981. Exponential sampling method for light scattering polydispersity analysis. *Opt. Acta*. 28:1059–1070.

Pansu, R. B. 1990. Kinetic versus thermodynamic control of DODAC vesicles formation. *New J. Chem.* 14:365–371.

Poste, G. 1980. The interaction of lipid vesicles (liposomes) with cultured cells and their use as carriers for drugs and macromolecules. *In* Liposomes in Biological Systems. G. Gregoriadis and A. C. Allison, editors. Wiley, New York. 101–151.

Roessner, D., and W. M. Kulicke. 1994. On-line coupling of flow field-flow fractionation and multiangle laser light scattering. *J. Chromatogr. A.* 687:249–258.

Rotenberg, M., and D. Lichtenberg. 1990. What determines the size of phospholipid vesicles made by detergent-removal techniques? *J. Colloid Interface Sci.* 144:591–594.

Tenchov, B. G., and T. K. Yanev. 1986. Weibull distribution of particle sizes obtained by uniform random fragmentation. *J. Colloid Interface Sci.* 111:1–7.

Tenchov, B. G., T. K. Yanev, M. G. Tihova, and R. D. Koynova. 1985. A probability concept about size distributions of sonicated lipid vesicles. *Biochim. Biophys. Acta.* 816:122–130.

Thielking, H., and W.-M. Kulicke. 1996. On-line coupling of flow field-flow fractionation and multiangle laser light scattering for the characterization of macromolecules in aqueous solution as illustrated by sulfonated polystyrene samples. *Anal. Chem.* 68:1169–1173.

Thielking, H., D. Roessner, and W.-M. Kulicke. 1995. On-line coupling of flow field-flow fractionation and multiangle laser light scattering for the characterization of polystyrene particles. *Anal. Chem.* 67:3229–3233.

van Zanten, J. H. 1994. Unilamellar vesicle diameter and wall thickness determined by Zimm's light scattering technique. *Langmuir.* 10: 4391–4393.

van Zanten, J. H. 1996. Characterization of vesicles and vesicular dispersions via scattering techniques. *In* Vesicles. M. Rosoff, editor. Marcel Dekker, New York. 239–294.

van Zanten, J. H., D. S.-W. Chang, I. Stanish, and H. G. Monbouquette. 1995. Selective extraction of Pb^{2+} by metal-sorbing vesicles bearing ionophores of a new class. *J. Membr. Sci.* 99:49–56.

van Zanten, J. H., and H. G. Monbouquette. 1991. Characterization of vesicles by classical light scattering. *J. Colloid Interface Sci.* 146: 330–336.

van Zanten, J. H., and H. G. Monbouquette. 1992. Biomimetic metal-sorbing vesicles: Cd^{2+} uptake by phosphatidylcholine vesicles doped with ionophore A23187. *Biotechnol. Prog.* 8:546–552.

van Zanten, J. H., and H. G. Monbouquette. 1994. Phosphatidylcholine vesicle diameter, molecular weight and wall thickness determined by static light scattering. *J. Colloid Interface Sci.* 165:512–518.

Walsh, A. J., and H. G. Monbouquette. 1993. Extraction of Cd^{2+} and Pb^{2+} from dilute aqueous solution using metal sorbing vesicles in a hollow-fiber cartridge. *J. Membr. Sci.* 84:107–121.

White, G., J. Pencer, B. G. Nickel, J. M. Wood, and F. R. Hallett. 1996. Optical changes in unilamellar vesicles experiencing osmotic stress. *Biophys. J.* 71:2701–2715.

Wittgren, B., and K.-G. Wahlund. 1997. Fast molecular mass and size characterization of polysaccharides using asymmetrical flow field-flow fractionation—multiangle light scattering. *J. Chromatogr. A.* 760: 205–218.

Wyatt, P. J., and D. N. Villalpando. 1997. High precision measurement of submicrometer particle size distributions. *Langmuir.* 13:3913–3914.

Zimm, B. H. 1948. The scattering of light and the radial distribution function of high polymer solutions. *J. Chem. Phys.* 16:1093–1099.